Ultrafast Cooling of Photoexcited Electrons in Gold Nanoparticle–Thiolated DNA Conjugates Involves the Dissociation of the Gold–Thiol Bond

3 AUTHORS:

Prashant K Jain
University of Illinois, Urbana-Champaign
63 PUBLICATIONS   8,994 CITATIONS

SEE PROFILE

Wei Qian
Georgia Institute of Technology
33 PUBLICATIONS   3,960 CITATIONS

SEE PROFILE

Mostafa A El-Sayed
Georgia Institute of Technology
675 PUBLICATIONS   54,870 CITATIONS

SEE PROFILE

Ultrafast Cooling of Photoexcited Electrons in Gold Nanoparticle–Thiolated DNA Conjugates Involves the Dissociation of the Gold–Thiol Bond

Prashant K. Jain, Wei Qian, and Mostafa A. El-Sayed*

Contribution from the Laser Dynamics Laboratory, School of Chemistry and Biochemistry, Georgia Institute of Technology, Atlanta, Georgia 30332−0400

Received October 10, 2005; E-mail: mostafa.el-sayed@chemistry.gatech.edu

Abstract: Using UV−visible extinction spectroscopy and femtosecond pump−probe transient absorption spectroscopy, we have studied the effect of femtosecond laser heating on gold nanoparticles attached to DNA ligands via thiol groups. It is found that femtosecond pulse excitation of the DNA-modified nanoparticles at a wavelength of 400 nm leads to desorption of the thiolated DNA strands from the nanoparticle surface by the dissociation of the gold−sulfur bond. The laser-initiated gold−sulfur bond-breaking process is a new pathway for nonradiative relaxation of the optically excited electrons within the DNA-modified gold nanoparticles, as manifested by a faster decay rate of the excited electronic distribution at progressively higher laser pulse energies. The experimental results favor a bond dissociation mechanism involving the coupling between the photoexcited electrons of the nanoparticles and the gold−sulfur bond vibrations over one involving the conventional phonon−phonon thermal heating processes. The latter processes have been observed previously by our group to be effective in the selective photothermal destruction of cancer cells bound to anti-epidermal growth factor receptor-conjugated gold nanoparticles.

I. Introduction

Noble metal nanoparticles are fascinating materials with great nanotechnological potential due to their unique and strongly size-dependent electronic, optical, physical, and chemical properties.[1,2] Additionally, the surfaces of nanoparticles can be easily functionalized with various organic and biomolecular ligands, among which the molecules with a sulfur headgroup are attracting considerable interest.[3] The strong affinity of sulfur to gold has been exploited to form molecular contacts, to link other species to the gold surface, or to form well-ordered self-assembled monolayers (SAMs)[4] for applications like surface patterning[5] and molecular electronics.[6] In the case of biomolecules, sulfur-containing cysteine and cystine amino acids, often found on the border of large proteins, have been employed to anchor proteins to gold nanoparticles, thus imparting the nanoparticles with essential biochemical functions like targeting, biocompatibility, etc.[7] Recent strategies[8,9] have employed alkanethiol-capped DNA oligonucleotides to link gold nanoparticle building blocks to form periodic functional assemblies, in addition to serving as efficient DNA detection schemes.

Recently, an interesting application of gold nanoparticles has emerged − as antennae for remote control of the activity of biomolecules bound to their surface. For instance, radio wave field-based induction heating of gold nanocrystals linked to DNA oligonucleotides in solution has recently been shown to dehybridize the DNA in a manner that is both reversible and specific.[10] More recently, research from our group has demonstrated the promising use of gold nanoparticles in spectroscopic and optical imaging-based cancer diagnostics,[11] as well as in immunotargeted laser photothermal cancer therapy.[12] This work was based on the surface plasmon enhancement of both absorption and scattering of gold nanoparticles. The observed tumor therapy is a result of the fact that the strongly enhanced absorption of light by immunotargeted gold nanoparticles is rapidly converted to heat on the picosecond time domain,[13] resulting in the heating of the neighboring cell surface, ultimately leading to cell death. It is thus obvious that the light absorbed by the gold nanoparticles is transferred to the antibody molecules and the cell environment by rapid electron−phonon relaxation in the nanoparticle followed by phonon−phonon relaxation,[13] resulting in an increase in the temperature of the cells.[14] In the present study, we aim to examine the rate, efficiency, and mechanism by which the light energy absorbed by gold nanoparticles is transferred to thiolated DNA ligands conjugated to the surface of the nanoparticle.

(1) Kelly, K. L.; Coronado, E.; Zhao, L. L.; Schatz, G. C. *J. Phys. Chem. B* **2003**, *107*, 668.
(2) Kreibig, U.; Vollmer, M. *Optical Properties of Metal Clusters*; Springer: New York, 1995.
(3) Nuzzo, R. G.; Allara, D. L. *J. Am. Chem. Soc.* **1983**, *105*, 4481.
(4) Ulman, A. *Chem. Rev.* **1996**, *96*, 1533.
(5) Xia, Y.; Rogers, J. A.; Paul, K. E.; Whitesides, G. M. *Chem. Rev.* **1999**, *99*, 1823.
(6) Joachim, C.; Gimzewski, J. K.; Aviram, A. *Nature* **2000**, *408*, 541.
(7) Katz, E.; Willner, I. *Angew. Chem., Int. Ed.* **2004**, *43*, 6042.
(8) Mirkin, C. A.; Letsinger, R. L.; Mucic, R. C.; Storhoff, J. J. *Nature* **1996**, *382*, 607.
(9) Nam, J.-M.; Stoeva, S. I.; Mirkin, C. A. *J. Am. Chem. Soc.* **2004**, *126*, 5932.

(10) Hamad-Schifferli, K.; Schwartz, J. J.; Santos, A. T.; Zhang, S.; Jacobson, J. M. *Nature* **2002**, *415*, 152.
(11) El-Sayed, I. H.; Huang, X.; El-Sayed, M. A. *Nano Lett.* **2005**, 5, 829.
(12) El-Sayed, I. H.; Huang, X.; El-Sayed, M. A. *Cancer Lett.* **2005**, in press.
(13) Link, S.; El-Sayed, M. A. *Annu. Rev. Phys. Chem.* **2003**, *54*, 331.
(14) Huang, X.; Jain, P. K.; El-Sayed, I. H.; El-Sayed, M. A. *Photochem. Photobiol.* **2006**, accepted for publication.

Due to their very high surface-to-volume ratios, nanoparticles are expected to show unique surface or interface effects[15] in their interaction with light and their photothermal properties. In correlation with surface or interfacial phenomena, the predominant role of nonequilibrium electrons in driving the most basic reactions, such as desorption, dissociation, or motion of molecules on metal surfaces, has been recently established.[16,17] To study similar phenomena in metal nanoparticles, the demonstrated ability of femtosecond pulse excitation to create nonequilibrium conditions[18] can be employed, and thus mechanism of nonradiative dynamical processes occurring on the nanoparticle surface can be determined.

In the present work, we employ UV−visible extinction spectroscopy and femtosecond pump−probe transient absorption spectroscopy to study the effect of photothermal heating of gold nanoparticles with surfaces modified by thiolated DNA. It is found that femtosecond pulse excitation of the nanoparticle−thiol conjugates initiated the cleavage of the surface gold−sulfur bond. Femtosecond transient absorption spectroscopy further revealed that bond-breaking serves as an additional mechanism for the relaxation of the optically excited electrons in the nanoparticle. The evolution of the bond-breaking can thus be indirectly followed in time by using ultrafast pump−probe transient absorption spectroscopy of the nanoparticles. The experimental results suggest that the surface bond dissociation does not result from a pure thermal heating of the irradiated nanoparticles resulting from phonon−phonon relaxation processes, but rather results from an ultrafast process driven by hot electrons of the nanoparticles.

II. Experimental Methods

A. Synthesis of Thiolated DNA-Modified Gold Nanoparticles. Gold nanoparticles (13.1 ± 1.3 nm) were prepared by the citrate reduction of chloroauric acid.[19] A self-assembled monolayer (SAM) of thiolated ss-DNA was formed on the surface of the gold nanoparticles by well-established procedures.[20] Typically, 2.4 nmol of purified 5′-SH-CH_2-CH_2-CH_2-CGC-ATT-CAG-GAT-3′ (Integrated DNA Technologies Inc.) was added to 1 mL of ~11 nM gold nanoparticle solution. After 24 h, the solution was brought to 0.1 M NaCl concentration and allowed to stand at room temperature for a further 40 h. The solution was then centrifuged at 12 400 rpm for 30 min. The supernatant was removed, and the reddish pellets at the bottom of the tube were dispersed in 1 mL of 0.1 M NaCl, 10 mM sodium phosphate buffer (pH 7) solution. This procedure was repeated, and the pellets at the bottom of the centrifuge tube were dispersed in 0.3 M NaCl, 10 mM sodium phosphate buffer (pH 7). The synthesized nanoparticle conjugates were characterized by UV−visible extinction (300−800 nm) on a Shimadzu UV-3101-PC spectrophotometer in transmission mode.

B. Laser Photothermal Heating of Thiolated DNA-Modified Gold Nanoparticles. A frequency-doubled Nd:vanadate laser (Coherent Verdi) was used as the pump for the Ti:sapphire laser system (Clark MXR CPA 1000), which generated laser pulses of 100 fs duration (fwhm) with energy of 1 mJ at 800 nm at a repetition rate of 1 kHz. The pump beam was mechanically chopped with a light beam chopper

(HMS 221).The second harmonic of the 800 nm fundamental at 400 nm was used for the optical heating of the DNA-modified gold nanoparticle solution placed in an optical cell (path length = 2 mm), kept under constant stirring. The diameter of the laser focus spot on the sample was 100 μm. The laser pump pulse energy used in the experiments was reduced to less than 250 nJ with neutral density filters. The solution was irradiated with various pulse energies ranging from 150 nJ/pulse to 24 μJ/pulse, for successive periods of 5 min each. The effect of optical heating on the sample was monitored by obtaining the UV−visible extinction at each pulse energy.

C. Femtosecond Electron Relaxation Dynamics of Thiolated DNA-Modified Gold Nanoparticles. Bigot et al.[21] and Melinger et al.[22] have already shown, using femtosecond pump−probe spectroscopy, the effect of the surrounding/embedding medium on the ultrafast electron relaxation dynamics in noble metal nanoparticles. To study the effect of the thiol modification of the gold nanoparticle surface on the electron relaxation dynamics, we employed femtosecond transient absorption spectroscopy.[23] In our work, 100 fs pulses (fwhm) at 400 nm (which were used for the optical heating) were used as the excitation source (pump). A white-light continuum, generated by focusing a small portion (4%) of the 800 nm fundamental beam of the Ti:sapphire laser onto a 1 mm sapphire plate, was used to probe the transient absorption of the sample at various delay times (*t*). The differential transmission signal *S*(*t*) was recorded with a pair of silicon photodiodes (Thorlab) and a lock-in amplifier (Stanford Research Systems). The recorded signal *S*(*t*) can be expressed as

$$S(\lambda,t) = \Delta T/T = (I_{\lambda,t} - I_{\lambda,0})/I_{\lambda,0}$$

where $\Delta T/T$ is the % change in the transmission of probe light, $I_{\lambda,t}$ is the intensity of the probe light at wavelength λ after a delay time *t* from the pump laser heating pulse, and $I_{\lambda,0}$ is the intensity of the probe light at λ without the pump. As a result, the recorded signal $S(\lambda,t)$ represents a transient bleach, which results from the optical excitation of the free electron distribution within the nanoparticles. Following this procedure, the electron relaxation dynamics of thiolated DNA-modified gold nanoparticles was measured for different pump pulse energies ranging from 30 to 900 nJ/pulse (low fluence regime) and compared with the dynamics in unmodified gold nanoparticles under similar aqueous solution conditions. The probe wavelength was set at the absorption maximum for both samples. The concentrations of the thiol modified and unmodified nanoparticle solutions were adjusted such that both solutions had a similar absorbance at the pump wavelength, i.e., 400 nm, in order to ensure similar hot electron excitation in both samples and thus enable comparison of their electron relaxation dynamics.

III. Results and Discussion

A. UV−Vis Extinction of Thiolated DNA-Modified Gold Nanoparticles. The UV−vis extinction spectra (300−800 nm) of thiolated DNA-modified gold nanoparticles and unmodified gold nanoparticles are shown in Figure 1. As evidenced by the spectra, the formation of a SAM of thiolated DNA on the gold nanoparticle surface by gold−sulfur bonding caused a shift in the surface plasmon absorption peak from 519 to 525 nm. Surface plasmon absorption properties are generally discussed within the framework of the Drude model,[24] according to which the plasmon peak position ($\lambda_{\text{sp max}}$) depends on the dielectric

(15) Del Fatti, N.; Flytzanis, C.; Vallée, F. *Appl. Phys. B* **1999**, *68*, 433.
(16) Petek, H.; Weida, M. J.; Nagano, H.; Ogawa, S. *Science* **2000**, *288*, 1402.
(17) Wolf, M.; Ertl, G. *Science* **2000**, *288*, 1352.
(18) Hodak, J. H.; Henglein, A.; Hartland, G. V. *J. Phys. Chem. B* **2000**, *104*, 9954.
(19) Turkevich, J.; Stevenson, P. C.; Hillier, J. *Discuss. Faraday Soc.* **1951**, *11*, 55.
(20) Mirkin, C. A.; Letsinger, R. L.; Mucic, R. C.; Storhoff, J. J. *Nature* **1996**, *382*, 607.

(21) Bigot, J.-Y.; Halte, V.; Merle, J.-C.; Daunois, A. *Chem. Phys.* **2000**, *251*, 181.
(22) Melinger, J. S.; Kleiman, V. D.; McMorrow, D.; Grohn, F.; Bauer, B. J.; Amis, E. J. *J. Phys. Chem. A* **2003**, *107*, 3424.
(23) Logunov, S. L.; Volkov, V. V.; Braun, M.; El-Sayed, M. A. *Proc. Natl. Acad. Sci. U.S.A.* **2001**, *98*, 8475.
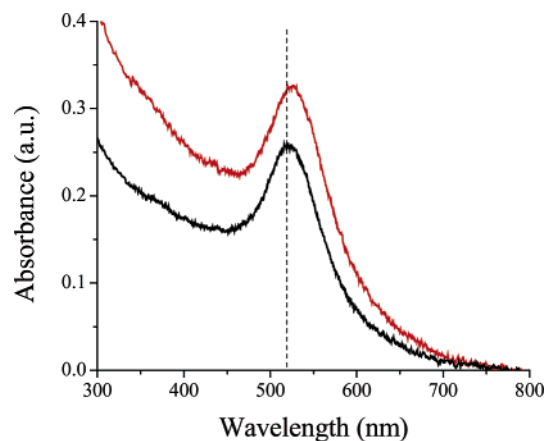(24) Mulvaney, P. *Langmuir* **1996**, *12*, 788.

Figure 1. UV−visible extinction spectrum of DNA-modified ∼13 nm Au NPs (red) and unmodified ∼13 nm gold nanoparticles (black) in the wavelength range 300−800 nm. The optical path length was 2 mm. The dashed black line is a guide to the eye, representing the extinction maximum at 519 nm for the unmodified gold nanoparticles.

constant of the surrounding medium (ϵ_m), as governed by

$$\lambda_{sp\,max}{}^2 = \lambda_p{}^2(\epsilon_\infty + 2\epsilon_m)$$

where ϵ_∞ is the high-frequency dielectric constant of gold due to interband and core transitions. λ_p is the bulk plasmon frequency of gold given by the following relation:

$$\lambda_p = 2\pi c/(Ne^2/m_e\epsilon_0)^{1/2}$$

where ϵ_0 is the permittivity in a vacuum, c is the speed of light in a vacuum, e is the electronic charge, N is the density of free electrons in the nanoparticle, and m_e is the effective mass of the electron. The red-shift in the plasmon wavelength resulting from the formation of the SAM can thus be attributed to a local increase in the medium refractive index as a result of the thiols[25] or to a change in the free electron density of the gold nanoparticle due to the strong surface coupling with sulfur.[26] Such shifts in the plasmon absorption maximum have been commonly employed in surface plasmon resonance (SPR)-based sensing of analytes.[27]

B. Femtosecond Pulse Heating of Thiolated DNA-Modified Gold Nanoparticles. Figure 2 shows the UV−visible extinction of the optically heated DNA-modified gold nanoparticle solution after 5 min heating periods at different pulse energies ranging from 150 nJ/pulse to 24 µJ/pulse. The figure shows that excitation of the thiolated DNA-modified gold nanoparticles with femtosecond pulses of increasing energy up to 2.74 µJ/pulse results in a gradual blue-shift in their plasmon extinction maximum from 525 to 519 nm, which is the plasmon maximum for unmodified gold nanoparticles (indicated by the dashed black line). This suggests that laser photothermal heating of the thiolated DNA-modified gold nanoparticles results in the dissociation of the gold−sulfur bond between the thiolated DNA strand and the nanoparticle surface. As shown in Figure 2 and the inset, the extent of the blue-shift (and thus the suggested bond dissociation) increases superlinearly with increasing
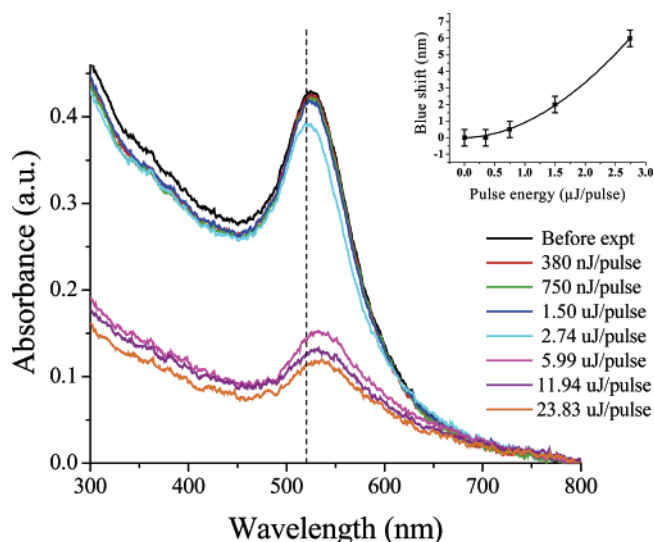
(25) Ghosh, S. K.; Nath, S.; Kundu, S.; Esumi, K.; Pal, T. *J. Phys. Chem. B* **2004**, *108*, 13963.
(26) Zhang, P.; Sham, T. K. *Phys. Rev. Lett.* **2003**, *90*, 245502.
(27) Van Duyne, R. P.; Hulteen, J. C.; Treichel, D. A. *J. Chem. Phys.* **1993**, *99*, 2101.

Figure 2. UV−visible extinction spectrum (300−800 nm) of thiolated DNA-modified gold nanoparticles after heating with 100 fs, 400 nm pulses for successive 5 min periods at pulse energies of 380 nJ/pulse, 750 nJ/pulse, 1.50 µJ/pulse, 2.74 µJ/pulse, 5.99 µJ/pulse, 11.94 µJ/pulse, and 23.83 µJ/pulse. The optical path length was 2 mm. The dashed black line is a guide to the eye, representing the extinction maximum at 519 nm for unmodified gold nanoparticles. The inset shows the blue-shift of the absorption maximum from an initial wavelength of 525 nm versus the excitation pulse energy up to 2.74 µJ/pulse. The solid black curve in the inset is a power law fit ($R = 0.9995$) to the data points, given by $y \propto x^{1.87\pm0.08}$. Error in estimating the blue-shift is 0.5 nm based on the step size in the absorbance scan.

excitation pulse energy. Higher optical pumping powers finally gave rise to a red-shifted, broadened, and diminished absorption. In other words, the nanoparticles finally aggregate when there are not enough surface ligands to stabilize/passivate the nano-particles in solution, thus resulting in the broadened and diminished absorption and bluish-purple precipitation of gold metal observed on the sides of the optical cell. The observed blue-shift on femtosecond excitation was fairly reproducible for three separate experimental batches (having similar absorbance at the excitation wavelength of 400 nm). The pulse energies at which the maximum blue-shift was observed were similar, ∼3 µJ/pulse for the different batches. Figure 3 shows a plot of the observed blue-shift in the plasmon maximum with the absorbed laser energy, based on data obtained from the different batches.

Figure 4 shows similar blue-shift of the surface plasmon maximum of ∼13 nm gold nanoparticles capped with mercap-toacetic acid (HS-CH$_2$COOH) on laser irradiation using 100 fs pulses. Note that the formation of the SAM of mercaptoacetic acid on the gold nanoparticle surface via gold−sulfur bonds shifts the extinction maximum from 519 nm for unmodified nanoparticles to 528 nm for the thiol-modified nanoparticles, the shift thus being larger than that in case of the thiolated DNA modification, possibly due to a tighter SAM for mercaptoacetic acid molecules. The SAM formation also leads to an observable broadening of the plasmon band of the nanoparticles, as attributed commonly to chemical interface damping.[2,28−30] Thus, on femtosecond pulse irradiation up to 3 µJ/pulse (Figure 4 and inset), the resulting blue-shift of the plasmon maximum from 528 to 521.5 nm, as well as the decrease in the plasmon band

(28) Persson, B. N. J. *Surf. Sci.* **1993**, *283*, 1993, 153.
(29) Hövel, H.; Fritz, S.; Hilger, A.; Kreibig, U. *Phys. Rev. B* **1993**, *48*, 18178.
(30) Bosbach, J.; Hendrich, C.; Stietz, F.; Vartanyan, T.; Trager, F. *Phys. Rev. Lett.* **2002**, *89*, 257404.
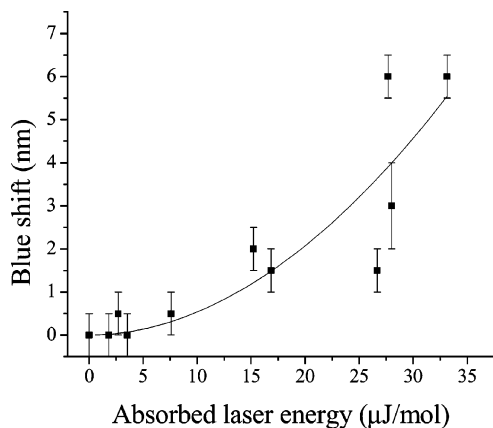
Figure 3. Observed blue-shift (nm) of the plasmon maximum versus the absorbed laser energy (μJ/mol). The data were obtained from three different batches of thiolated DNA-modified gold nanoparticles. The absorbed laser energy was calculated per mole of the nanoparticles in solution using the incident pulse energy in μJ/pulse, the solution absorbance at the excitation wavelength of 400 nm, the irradiation time of 5 min at each pulse energy, and the nanoparticle concentration in solution. The solid black curve is a power law fit ($R = 0.8718$) to the data points, given by $y \propto x^{1.95 \pm 0.80}$. Error in estimating the blue-shift is based on the step size in the absorbance scan.
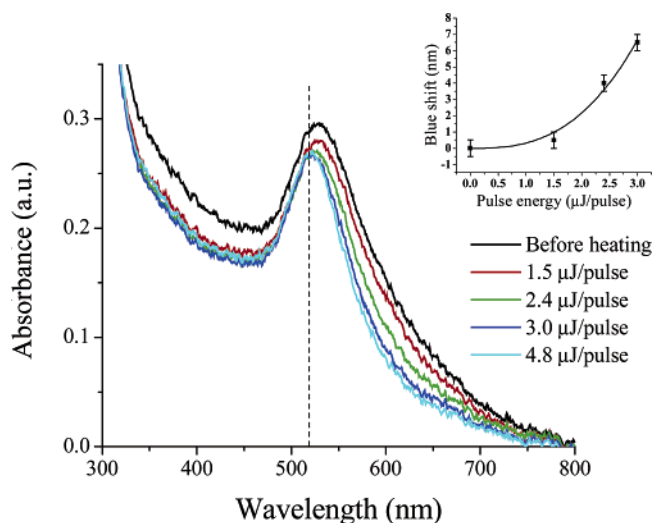

Figure 4. UV−visible extinction spectrum (300−800 nm) of mercaptoacetic acid-modified gold nanoparticles after heating with 100 fs, 400 nm pulses for successive 5 min periods at pulse energies of 1.5 μJ/pulse, 2.4 μJ/pulse, 3.0 μJ/pulse, and 4.8 μJ/pulse. The optical path length was 2 mm. The dashed black line is a guide to the eye, representing the extinction maximum at 519 nm for unmodified gold nanoparticles. The inset shows the blue-shift of the absorption maximum from an initial wavelength of 528 nm versus the excitation pulse energy up to 3 μJ/pulse. The solid black curve in the inset is a power law fit ($R = 0.9883$) to the data points, given by $y \propto x^{2.76 \pm 0.69}$. Error in estimating the blue-shift is 0.5 nm based on the step size in the absorbance scan.

fwhm from ∼140 to ∼100 nm, is clearly attributable to the gold−sulfur bond dissociation on the nanoparticle surface. Similar gold−sulfur bond dissociation in alkanethiolate SAMs on gold surfaces by STM-induced excitation and electron beam irradiation has been reported by Avouris et al.[31] and Chen et al.,[32] respectively.

C. Femtosecond Electron Relaxation Dynamics in DNA-Modified Gold Nanoparticles. Figure 5 shows a comparison

(31) Avouris, P.; Walkup, R. E.; Rossi, A. R.; Akpati, H. C.; Nordlander, P.; Shen, T. C.; Abeln, G. C.; Lyding, J. W. *Surf. Sci.* **1996**, *363*, 368.
(32) Chen, Y.; Palmer, R. E.; Shelley, E. J.; Preece, J. A. *Surf. Sci.* **2002**, *502/503*, 208.

of the transient bleaching dynamics of DNA-modified gold nanoparticles with unmodified gold nanoparticles for pump pulse energy ranging from 30 to 900 nJ/pulse. It is well known that the rise of the transient bleach signal is a result of electron−electron scattering within the nanoparticles, while the decay can be directly related to the dynamics of relaxation of excited/hot electrons by the process of electron−phonon coupling on the time scale of ∼1 ps and phonon−phonon coupling on longer time scales of ∼100 ps.[13] The rise and decay were fit to an exponential function[33] of the form

$$(1 - \exp(-t/\tau_{\mathrm{r}})) \exp(-t/\tau_{\mathrm{d}})$$

so as to obtain the rise time τ_{r} (ps) and the decay time or the hot electron lifetime τ_{d} (ps).

It can be seen from Figure 5 that, at a lower value of the pulse energy (38 nJ/pulse), the hot electron lifetimes of the DNA-modified gold nanoparticles ($\tau_{\mathrm{d}}'' = 1.04 \pm 0.04$ ps) and the unmodified gold nanoparticles ($\tau_{\mathrm{d}}' = 1.10 \pm 0.04$ ps) are similar. At progressively higher pulse energies, the electron relaxation in both DNA-modified and unmodified nanoparticles becomes slower as a result of the linear increase of the electronic heat capacity with the hot electron temperature.[34] However, with higher pulse energy, the electron relaxation rate in DNA-modified nanoparticles gets progressively faster than that in unmodified nanoparticles. As can be seen from the photothermal heating experiment described in section B, the femtosecond pulse excitation of the nanoparticle electrons initiates cleavage of the gold−sulfur bond; the extent of this bond-breaking process increases with increasing pump energy. Since a part of the energy of the hot electrons is utilized in the bond-breaking, an additional pathway is opened up for the electron energy relaxation in the DNA-modified nanoparticles. The electron relaxation in DNA-modified nanoparticles as compared to that in the unmodified nanoparticles is therefore progressively faster at progressively higher input pulse energies.

It is conceivable that the presence of the thiolated DNA ligands around the gold nanoparticle enhances the electronic relaxation of the latter. In other words, energy can be transferred to the DNA ligands, leading to an increase in the nanoparticle relaxation rate, and this energy can be used for the dissociation of the gold−sulfur bond on a later time scale. However, due to the large density of vibrational states in the DNA ligands, it would be unlikely for this transferred energy to be later localized in the gold−sulfur bond, leading to the dissociation. Hence, we believe that direct coupling between the hot electrons and the gold−sulfur bond is responsible for the bond-breaking process. Besides, the pulse energy dependence of the hot electron relaxation dynamics can be best explained by the femtosecond pulse-initiated dissociation of the gold−sulfur bond. The bond dissociation process could be indirectly followed in time by monitoring the ultrafast electron dynamics by using the femtosecond transient absorption spectroscopy. The gold−sulfur bond-breaking cannot be attributed to a conventional thermal heating of the irradiated nanoparticles. Conventional heating takes place by phonon−phonon relaxation which occurs on a much longer time scale, typically ∼100 ps.[13] The occurrence

(33) Averitt, R. D.; Westcott, S. L.; Halas, N. J. *Phys. Rev. B* **1998**, *58*, R10203.
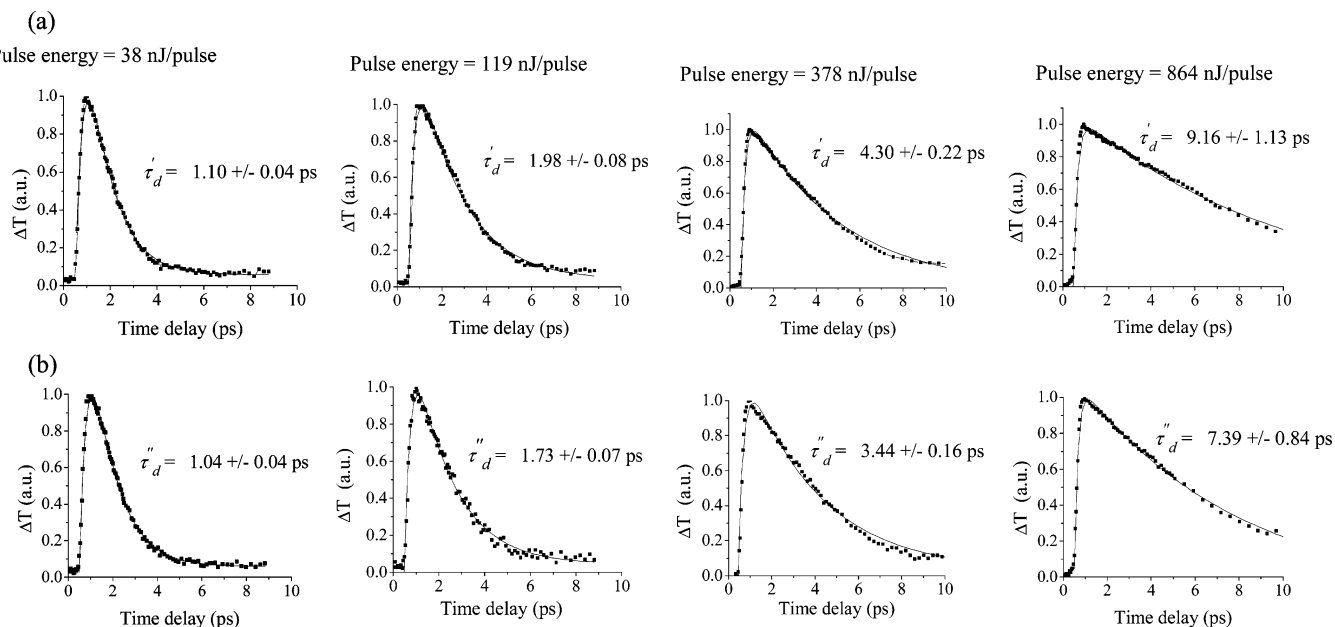(34) Ashcroft, N. W.; Mermin, N. D. *Solid State Physics*; Harcourt Brace: Orlando, 1976.

(a)

(b)

Figure 5. Femtosecond transient bleaching in (a) unmodified gold nanoparticles and (b) thiolated DNA-modified gold nanoparticles, pumped with 100 fs, 400 nm pulses at energies of 38, 119, 378, and 864 nJ/pulse, and probed at their respective absorption maximum. The rise and decay of the transient bleaching are fit to the exponential function $(1 - \exp(-t/\tau_r)) \exp(-t/\tau_d)$ to obtain the hot electron relaxation times τ_d' in unmodified gold nanoparticles and τ_d'' in DNA-modified gold nanoparticles. The errors in the hot electron relaxation times are those obtained from the fitting.

of bond-breaking on the electron−phonon coupling time scale (typically within ∼1 ps for gold) suggests a hot-electron-initiated process rather than one that involves a phonon heat bath as the energy source. It has also been established recently that the nonequilibrium between electrons and phonons created by ultrashort pulse excitation generally favors nonconventional electron-mediated reaction pathways.[35]

D. Time Evolution of the Bond-Breaking Process. A mechanism of desorption of ligands from a metal substrate, driven by highly excited local surface vibrational modes (surface phonons or metal−adsorbate bond vibrations) thermally equilibrated with hot electrons, has been proposed in surface science.[36] The rate of desorption by such a mechanism is expected to go as $\exp(-E_d/k_B T_e)$,[37] where E_d is the activation barrier for the metal−adsorbate bond dissociation and T_e is the temperature of the hot electron bath. To verify the presence of such a mechanism, we modeled the time evolution of the laser-initiated bond-breaking in terms of the electron relaxation dynamics in the nanoparticles. The dynamics of the electron relaxation process in gold nanoparticles is generally described by the two-temperature model (TTM)[38] as

$$c_e \frac{dT_e}{dt} = -G(T_e - T_l) \quad (1)$$

where c_e is the electronic heat capacity ($c_e = 66T_e$ J m^{-3} K^{-1}),[27] T_e is the electronic temperature (K), T_l is the lattice temperature (K), t represents the time (s), G is the electron−phonon coupling constant (W m^{-3} K^{-1}), and the temporal profile of the pulse and the thermal conduction term[39] have been neglected in the

equation. We further modified the TTM model for the DNA-modified particles by incorporating the additional relaxation pathway due to the bond-breaking process (assumed first-order) as

$$c_e \frac{dT_e}{dt} = -G(T_e - T_l) - R(T_e)\Delta H \quad (2)$$

$$R(T_e) = k(T_e)[\text{Au−S}] \quad (3)$$

where ΔH is the enthalpy for the gold−sulfur bond dissociation (155 kJ mol^{-1}),[40] R is the rate of gold−sulfur bond dissociation (mol m^{-3} s^{-1}), k is the first-order rate constant of gold−sulfur bond-breaking (s^{-1}), and [Au−S] is the gold−sulfur bond concentration (∼300 mol m^{-3}). Thus, this simple model based on eqs 1−3 incorporates two experimental trends: first, the electron−phonon relaxation dynamics getting slower in both DNA-modified and unmodified nanoparticles at higher powers due to the dependence of the electronic heat capacity on the pulse power ($c_e = 66T_e$), and second, the additional energy relaxation channel due to the bond-breaking in DNA-modified nanoparticles increasing in contribution with higher pulse energies ($k = f(T_e)$). The first-order decay dynamics in the unmodified nanoparticles can be described as $T_e = T_{e,0} \exp(-t/\tau_d')$ and hence,

$$\frac{dT_e}{dt} = -\frac{T_e}{\tau_d'} \quad (4)$$

where $T_{e,0}$ is the peak electronic temperature. Similarly for DNA-modified nanoparticles,

(35) Hamers, R. J. *Surf. Sci.* **2005**, *583*, 1.
(36) Budde, F.; Heinz, T. F.; Kalamarides, A.; Loy, M. M. T.; Misewich, J. A. *Surf. Sci.* **1993**, *283*, 143.
(37) Prybyla, J. A.; Tom, H. W. K.; Aumiller, G. D. *Phys. Rev. Lett.* **1992**, *68*, 503.
(38) Sun, C. K.; Vallee, F.; Acioli, L. H.; Ippen, E. P.; Fujimoto, J. G. *Phys. Rev. B* **1994**, *50*, 15337.

(39) Bauer, C.; Abid, J.-P.; Fermin, D.; Girault, H. H. *J. Chem. Phys.* **2004**, *19*, 15.
(40) Ramachandran, G. K.; Hopson, T. J.; Rawlett, A. M.; Nagahara, L. A.; Primak, A.; Lindsay, S. M. *Science* **2003**, *300*, 1413.

$$\frac{dT_e}{dt} = -\frac{T_e}{\tau_d''} \tag{5}$$

Substituting (4) and (5) in (1) and (2) respectively, subtracting (2) from (1), and using (3),

$$k(T_e) = \frac{c_e T_e}{[Au-S]\Delta H}\left(\frac{1}{\tau_d''} - \frac{1}{\tau_d'}\right)$$

Using the dependence of the electronic heat capacity on the electronic temperature for gold ($c_e = 66T_e$ J m^{-3} K^{-1}), substituting the values of ΔH and [Au$-$S], the bond dissociation rate constant k at the peak electronic temperature can be obtained as

$$k = \frac{1.47 \times 10^{-6} T_{e,0}^{\,2}}{\tau_{bb}}$$

where

$$\tau_{bb} = \left(\frac{1}{\tau_d''} - \frac{1}{\tau_d'}\right)^{-1}$$

can be viewed as the time constant for the bond dissociation process and can be calculated from the experimental hot electron lifetimes for the two different samples obtained from Figure 5. The peak electronic temperatures were calculated for different pulse energies as per the method in an earlier reference.[41] The calculated rate constants k have been plotted against the pulse energy in Figure 6a. The plot of the calculated bond-breaking rate constant k with the pulse energy shows a superlinear trend, similar to the plot of the blue-shift of the surface plasmon absorption versus the laser pulse energy. The superlinear dependence ($y \propto x^{1.43}$) of the bond dissociation rate constant on the pulse energy eliminates the possibility of direct one-photon electronic excitation of the thiol adsorbate.

Figure 6b shows a plot of $\ln(hk/k_bT_e)$ versus $1/T_e$, which demonstrates that the estimated kinetics of the bond-breaking satisfies the activated Eyring rate process with respect to the electronic temperature T_e. In other words, $k \propto \exp(-E_d/k_bT_e)$. This strongly supports hot-electron-initiated cleavage of the gold$-$sulfur bonds, suggested in section C. The activation energy E_d for the dissociation (with respect to an electronic temperature) is calculated to be 10.3 kJ/mol (0.1 eV) from the Eyring plot. A previous measurement by Ramachandran et al.,[40] based on conductivity switching in thiol SAMs on a gold surface, yielded a similar value. The low activation barrier of 0.1 eV (as compared to the gold$-$sulfur bond dissociation energy of 1.6 eV) has been suggested to be a consequence of weakened bonds between gold atoms attached to the sulfur and neighboring gold atoms.[42]

A hot-electron-initiated bond dissociation mechanism involving the population of antibonding states of metal$-$adsorbate bonds lying above the metal Fermi level by excited conduction electrons is well known in the literature[43] and may explain the trend of k with the excitation pulse energy. However, the antibonding orbital of the gold$-$sulfur bond has been calculated
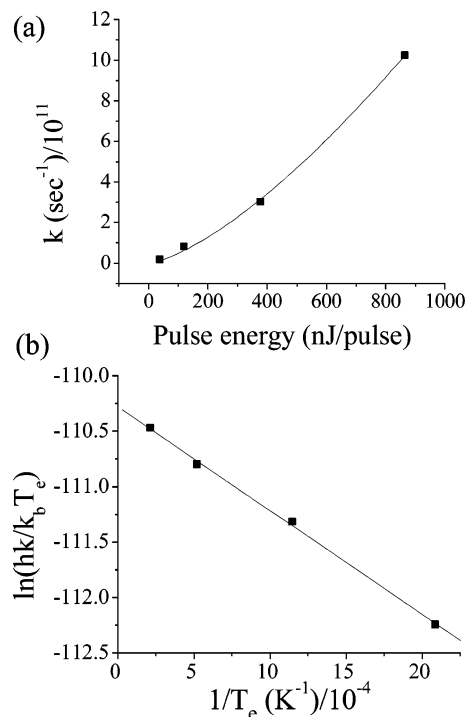
Figure 6. (a) Plot of the calculated gold$-$sulfur bond-breaking rate constant k (s^{-1})/10^{11} against the excitation pulse energy (nJ/pulse). The curve is a power law fit ($R = 0.9995$) to the experimental data having the form $y \sim x^{1.43 \pm 0.06}$. (b) Eyring plot of $\ln(hk/k_bT_e)$ versus $1/T_e$ (K^{-1})/10^{-4}. The solid line is a straight line fit ($R = -0.99922$) to the data given by $y = -936.5x - 110.3$, yielding $\Delta H_d/R = 0.9365$ K and $\Delta S_d/R = -0.1103$.

to be 0.64 eV below the Fermi level of gold.[44] Nevertheless, the orbital energy distribution for the gold$-$sulfur bond may not be known well enough to eliminate such a mechanism. Alternatively, surface phonons of the nanoparticle initiated by the hot electrons may also drive dissociation by weakening the surface$-$ligand bonds through vibrations.[45,46]

E. Efficiency of the Laser-Initiated Bond-Breaking Process. The thermodynamic efficiency of the laser-initiated bond-breaking process (η) can be calculated as

$$\eta = W/Q$$

where Q is the absorbed laser energy and W is the amount of energy required to break all the gold$-$sulfur bonds within the optical cell of volume 0.63 cm^3. On the basis of an optical density of 0.42 for the sample (i.e., a gold nanoparticle concentration of 7.8 nM) and a bond dissociation energy of 155 $\times$ 10^3 J mol^{-1} for the gold$-$sulfur bond, and assuming 220 DNA strands per $\sim$13 nm nanoparticle,[47] W is estimated to be 0.17 mJ. Figure 2 indicates that the maximum blue-shift (and thus the maximum gold$-$sulfur bond dissociation) occurs at a pulse energy of $\sim$3 μJ/pulse, or an absorbed energy of 1.46 μJ/pulse based on an absorbance of 0.29 at 400 nm. For this pulse energy and a pulse repetition rate of 1 kHz, the laser energy Q absorbed by the solution in the 5 min irradiation time was estimated to be 0.44 J. Consequently, an upper limit on

(41) Averitt, R. D.; Westcott, S. L.; Halas, N. J. *J. Opt. Soc. Am. B* **1999**, *16*, 1814.
(42) Felice, R. D.; Selloni, A.; Molinari, E. *J. Phys. Chem. B* **2003**, *107*, 1151.
(43) Bonn, M.; Funk, S.; Hess, C.; Denzler, D. N.; Stampf, C.; Scheffler, M.; Wolf, M.; Ertl, G. *Science* **1999**, *285*, 1042.

(44) Beardmore, K. M.; Kress, J. D.; Gronbech-Jensen, N.; Bishop, A. R. *Chem. Phys. Lett.* **1998**, *286*, 40.
(45) Trenhaile, B. R.; Antonov, V. N.; Xu, G. J.; Nakayana, K. S.; Weaver, J. H. *Surf. Sci.* **2005**, *583*, L135.
(46) Watanabe, K.; Kato, H.; Matsumoto, Y. *Surf. Sci. Lett.* **2000**, *446*, L134.
(47) Demers, L. M.; Mirkin, C. A.; Mucic, R. C.; Reynolds, R. A.; Letsinger, R. L.; Elghanian, R.; Viswanadham, G. *Anal. Chem.* **2000**, *72*, 5535.

the efficiency η at this pulse energy is calculated to be $\sim 4 \times 10^{-4}$. Insight into the low value of this efficiency can be obtained by analyzing the mechanism of the hot electron relaxation, the source of bond-breaking.

Relaxation of the hot electron gas in nanoparticles is believed to occur through two different channels: bulk electron−phonon interactions and electron−surface interactions.[48] The latter process occurs by coupling between the electrons and two kinds of surface phonon modes, namely acoustic and capillary surface modes. Thus, the effective electron−phonon coupling constant is determined by summing the different contributions:

$$G_{eff} = G_{bulk} + G_a + G_c$$

where G_{bulk} is the bulk contribution, measured to be $\sim 2.95 \times 10^{16}$ W m^{-3} K^{-1} by Groenveld et al.[49] G_a and G_c stand for the acoustic and capillary surface mode coupling terms, respectively, given by Belotskii et al.[48] as

$$G_c = \left(\frac{3}{16\pi}\right) k_B \left(\frac{v_f}{R}\right) n \left(\frac{m_e \omega_1^2}{\sigma}\right)\left(\frac{V_0}{\varphi_0}\right)^2$$

and

$$G_a = \left(\frac{1}{16\pi}\right) k_B \left(\frac{v_f}{R^2}\right) n \left(\frac{m_e}{\rho}\right)\left(\frac{\omega_D}{c_1}\right)^2\left(\frac{V_0}{\varphi_0}\right)^2$$

where k_B is Boltzmann's constant (1.38×10^{-23} J K^{-1}), n is the free electron density for gold (5.9×10^{28} m^{-3}), m_e is the electron mass (9.1×10^{-31} kg), σ is the surface tension of solid gold (2×10^{-3} N/m), φ_0 is the work function of gold (4.7 eV), V_0 is the Fermi energy (5.5 eV), v_f is the Fermi velocity (1.4×10^6 ms^{-1}), R is the nanoparticle radius (6.5 nm), ω_D is the Debye frequency (2.2×10^{13} s^{-1}), ρ is the density of gold (19 300 kg m^{-3}), and c_1 is the longitudinal speed of sound in gold (3240 ms^{-1}). ω_1 is the maximum frequency of the capillary modes,

$$\omega_1 = \sqrt{\frac{\sigma}{\rho R^3} l(l-1)(l+2)}$$

where l is the angular momentum number corresponding to the shortest possible surface wave, which is given by the integer part of $\pi R/d$, where d is the lattice parameter for gold, i.e., 4 Å. Accordingly, the contribution of the surface modes ($G_a + G_c$) to the electronic relaxation of the ~ 13 nm gold nanoparticles is estimated to be 3.34×10^{14} W m^{-3} K^{-1}, i.e., $\sim 10^{-2}$ times the net electron−phonon coupling constant G_{eff}.

The low energy efficiency of the bond-breaking process may thus be accounted for by the small contribution of the gold nanoparticle surface to the hot electron relaxation, in the cae of a mechanism where surface phonon modes initiated by the photoexcited excited electrons of the nanoparticle drive the cleavage of the surface gold−sulfur bonds. There have been several studies in the past by our group[25] and others[50] to measure the contribution of surface phonon scattering in gold nanoparticles to the electron−phonon relaxation. It was found that the relaxation rate was independent of shape or size down to a

nanoparticle diameter as small as 3 nm (electronic mean free path in gold = 40 nm). Hartland and co-workers have shown that the contribution of electron−surface phonon scattering to the overall electron−phonon scattering cross section is very small due to the small number of valence electrons in gold (only one electron) combined with a large atomic mass.[50] However, in the present study, the hot electron energy lost to the surface modes, although small in contribution, might be detected by the dissociation of the gold−sulfur bonds on the nanoparticle surface. The resulting bond dissociation is concluded experimentally from the observed changes in the plasmon absorption as well as the increase in the transient bleach decay rate.

F. Photothermal Excitation of Gold Nanoparticle−Protein Conjugates. The effect of femtosecond excitation on thiolated DNA-modified gold nanoparticles can be compared with the photothermal laser heating of gold nanoparticle−protein conjugates. In a previous work,[14] we studied the photothermal destruction of biological cells enriched with anti-epidermal growth factor receptor (EGFR)-conjugated ~ 40 nm gold nanoparticles on exposure to continuous wave laser radiation at 514 nm. To estimate the local temperature rise within the cells as a result of the exposure of the gold nanoparticle−antibody conjugates to a particular laser power, we used a numerical heat transport model. The model assumed photothermal conversion of absorbed laser energy into heat by an equilibrium thermal heating process (occurring by phonon−phonon relaxation). Our numerically estimated threshold temperatures of 70−80 °C for the photothermal destruction of the cells agreed with the measured threshold temperature for destruction of the cells by oven-heating and those measured in earlier measurements,[51] thus validating the model. The nanoparticle-mediated simple photothermal heating of cells is in sharp contrast to the femtosecond-pulse-initiated desorption taking place in the present study. In case of the thiolated DNA ligands, bound covalently to the gold surface, the energy of the nonequilibrium hot electrons is coupled into the weak surface gold−sulfur bonds. However, in case of the anti-EGFR-conjugated gold nanoparticles, the antibody molecules are held to the gold surface by a number of noncovalent interactions[52] and do not provide an additional channel for energy dissipation. Consequently, energy relaxation is attained by conventional phonon−phonon cooling within the gold nanoparticles and the surrounding cell medium, leading to a temperature rise in direct proportion to the laser energy.[14]

IV. Conclusions

We found that exposure of thiolated DNA-modified gold nanoparticles to femtosecond laser pulses led to the desorption of the thiolated DNA strands from the nanoparticle surface by breaking the gold−sulfur bond, as evidenced by the changes in the nanoparticle surface plasmon absorption band. The bond-breaking process led to an observed increase in the rate of the excited electron relaxation in the DNA−modified nanoparticles. Thus we were able to follow the time evolution of gold−sulfur bond dissociation by femtosecond transient absorption spectroscopy of the thiolated DNA−modified gold nanoparticles. The experimental results suggest that the rapid surface bond

(48) Belotskii, E. D.; Tomchuk, P. M. *Int. J. Electron.* **1992**, *73*, 955.
(49) Groenveld, R. H. M.; Sprik, R.; Lagendijk, A. *Phys. Rev. Lett.* **1990**, *64*, 784.
(50) Hodak, J. H.; Henglein, A.; Hartland, G. V. *J. Chem. Phys.* **2000**, *112*, 5942.

(51) Hirsch, L. R.; Stafford, R. J.; Bankson, J. A.; Sershen, S. R.; Rivera, B.; Price, R. E.; Hazle, J. D.; Halas, N. J.; West, J. L. *Proc. Natl. Acad. Sci. U.S.A.* **2003**, *100*, 13549.
(52) Sokolov, K.; Follen, M.; Aaron, J.; Pavlova, I.; Malpica, A.; Lotan, R.; Richards-Kortum, R. *Cancer Res.* **2003**, *63*, 1999.

dissociation does not result from a pure thermal heating of the irradiated nanoparticles, but rather is initiated by the photoexcited electrons of the nanoparticle, possibly via electronic coupling to the surface gold−sulfur bond vibrations or the nanoparticle surface phonons. Hot-electron-mediated chemistry on metal surfaces is well established in surface science; our experimental findings extend these ideas to the realm of nanoparticles, where the surface is of the utmost importance.[11] The behavior of the covalently bound thiolated DNA ligands on exposure to femtosecond pulses is contrasted with the photothermal laser excitation of anti-EGFR-conjugated gold nanoparticles, where a local temperature rise results from the conversion of light to heat by phonon−phonon relaxation processes in the nanoparticle.

JA056769Z